Performance Analysis of Cooperative Communication in Decentralized Wireless Networks with Unsaturated Traffic

Yong Zhou, *Member, IEEE*, and Weihua Zhuang, *Fellow, IEEE*

***Abstract*—In this paper, we investigate the performance of cooperative communication in decentralized wireless networks under unsaturated traffic conditions with randomly positioned single-hop source-destination pairs and relays, where interference is the main performance-limiting factor. The traffic unsaturation and concurrent cooperative transmissions introduce a correlation between the interferer density and the packet retransmission probability, and a correlation of interference power in both space and time domains, which complicate the interference characterization. Based on queueing theory and stochastic geometry, the stationary interferer density is derived by solving a fixed-point equation, which is proved to have a unique solution. According to the relay selection scheme, we characterize the correlation of interference power in two consecutive time-slots by identifying the densities of source and relay retransmissions. Based on the interferer density and interference correlation, we derive the outage probability and average packet delay of the cooperative scheme, while taking into account the dynamic traffic arrivals, interference correlation, relay selection scheme, and spatial node distribution. The performance analysis is validated by extensive simulations. The analytical results provide useful insights on cooperative communication in large-scale networks.**

***Index Terms*—Poisson point process, decentralized wireless networks, unsaturated traffic, interference correlation, cooperative communication.**

I. Introduction

Decentralized wireless networks have recently attracted extensive attentions due to their low deployment costs and promising applications (e.g., reliable sensing data transmission and timely alert information dissemination in flood-prone areas). Because of the spectrum scarcity, supporting concurrent transmissions across a network is necessary to enhance spectrum utilization by exploiting the spatial frequency reuse gain. However, due to the broadcast nature of wireless communications, signals transmitted from all unintended transmitters constitute co-channel interference observed by a receiver, which has a detrimental effect on the packet reception. As the main performance-limiting factor, accurate characterization of co-channel interference is a fundamental step towards understanding the overall performance of decentralized wireless networks.

The co-channel interference can be approximated by a Gaussian random process for tractability in performance analysis [1]. However, the Gaussian approximation does not completely characterize the co-channel interference, as it depends on many factors, including the interferer distribution, medium access probability, traffic pattern, and propagation channel. Stochastic geometry [2], [3] as a powerful tool can be used to model random node locations in decentralized wireless networks. Via modeling the spatial locations of concurrent transmitters as a homogeneous Poisson point process (PPP), the co-channel interference at any time instant can be characterized, which allows for accurate performance evaluation for both direct transmissions [4], [5] and cooperative transmissions [6]–[10]. In particular, such a performance analysis framework is applied to a cooperative spectrum sharing network in [6], which shows that the spectrum efficiency can be enhanced by exploiting the spatial diversity gain. By forming a primary exclusive region to eliminate the dominant interference, the authors in [7] derive the outage probabilities for different location-based relay selection schemes. Altieri *et al.* propose a random relay activation strategy for a decentralized wireless network in [8], where each relay operates in full-duplex mode. The outage probability is analyzed for Rayleigh fading channels to investigate the tradeoff between the cooperation gain and the additional interference due to relay transmissions. However, these studies focus on the scenario where the source nodes always have packets to transmit (i.e., a saturated traffic condition) under the assumption that the interference power observed at adjacent locations and in consecutive time-slots is independent.

The packet delivery probability and spatial network throughput of direct transmissions in decentralized wireless networks with unsaturated traffic are derived in [11] and [12], respectively. In addition, the authors in [13] study the impact of the number of packet retransmissions on the overall performance of different medium access control (MAC) schemes in an interference-limited Poisson network with unsaturated traffic. Under the queue stability constraint, the stable throughput of different cooperative strategies is analyzed for fixed topology networks [14], [15], which cannot be directly extended to the scenario with random node locations. On the other hand, the authors in [16]–[19] study the impact of interference correlation on the performance of direct transmissions. The authors

This research was supported in part by Natural Sciences and Engineering Research Council (NSERC) of Canada and NSERC Strategic Network FloodNet. This work was carried out while the first author was a PhD student at the University of Waterloo, Canada.

Y. Zhou is with the Department of Electrical and Computer Engineering, University of British Columbia, Vancouver, BC, V6T 1Z4, Canada (E-mail: y233zhou@uwaterloo.ca).

W. Zhuang is with the Department of Electrical and Computer Engineering, University of Waterloo, Waterloo, ON, N2L 3G1, Canada (E-mail: wzhuang@uwaterloo.ca).

in [16] investigate three main factors that affect interference correlation, i.e., node locations, traffic pattern, and propagation channel. For different combinations of these influential factors, the correlation coefficients of interference power in two consecutive time-slots are derived. Considering the interference correlation due to node locations in [17], [18] and traffic pattern in [19], the authors derive the outage probabilities of direct transmissions and show that the interference correlation reduces the packet delivery probability. Such a performance analysis framework is extended to derive the packet delivery probability of a cooperative transmission in a Poisson field of interferers in [20]–[22], while taking into account the correlation of interference power observed by the relay and destination nodes. By assuming the same set of interferers during the transmission periods of the source and relay nodes, these studies focus on a saturated traffic scenario where only one source-destination pair is activating the cooperative transmission (i.e., without concurrent cooperative transmissions), and cannot characterize the overall network performance. In addition, an opportunistic cooperative scheme is proposed in [23] for a wireless ad hoc network with saturated traffic, leading to a mixture of direct and cooperative transmissions and considering the interference redistribution due to relay transmissions.

Different from the aforementioned studies, we consider unsaturated traffic and concurrent cooperative transmissions in a decentralized wireless network, where interference power exhibits statistical dependence at adjacent locations and in consecutive time-slots. The traffic unsaturation and concurrent cooperative transmissions complicate the characterization of both the interferer density and the interference correlation. Specifically, the interferer density depends on the traffic arrival rate and affects the packet retransmission probability. In addition, the packet retransmission probability affects the packet service rate and in turn affects the probability of having an empty queue and the interferer density. Such a correlation should be considered when characterizing the interferer density. On the other hand, as each (interfering) relay is geographically close to its intended source node, the interference power observed by a destination node in two consecutive time-slots is correlated. Similarly, the interference power observed by a destination node and its neighboring relays in the same time-slot is also correlated. The spatial and temporal correlation of interference power leads to the correlation of successful packet receptions at adjacent locations and in consecutive time-slots. The level of interference correlation depends on the packet retransmission probability as well as the relay selection scheme, which should be considered when characterizing the interference correlation.

In this paper, we study the performance of a cooperative truncated automatic repeat request (ARQ) scheme in a decentralized wireless network with unsaturated traffic and randomly positioned single-hop source-destination pairs and relays. Upon the transmission failure of a direct link, a potential relay with the best channel quality to the destination node and having successfully received the packet from the source node is selected to retransmit the packet. We derive the stationary interferer density by establishing and solving a fixed-point equation, which captures the correlation between the interferer density and the packet retransmission probability. The fixed-point equation is proved to have a unique solution according to Contraction Mapping Theorem. In addition, a sufficient condition for a stable queue at all source nodes is presented. The correlation of node locations, due to packet retransmissions, induces the correlation of interference power. Based on the interference correlation, we derive the outage probability and average packet delay of the cooperative truncated ARQ scheme.

The main contributions of this paper are three-fold:

1) We develop a theoretical performance analysis framework for cooperative communication in a decentralized wireless network with unsaturated traffic and correlated interference power. It is shown that the performance analysis under the assumption of independent interference power overestimates the network performance. The analytical framework provides a better understanding of the benefits of cooperative communication in decentralized wireless networks;

2) Based on stochastic geometry and queueing theory, we characterize the interference power from two aspects, i.e., stationary interferer density and interference correlation in two consecutive time-slots. The stationary interferer density is derived by utilizing its relationship to the packet retransmission probability, while the interference correlation is characterized by deriving the densities of source and relay retransmissions;

3) We derive the outage probability and average packet delay of the cooperative truncated ARQ scheme in terms of important network and protocol parameters. The analytical results can be used to evaluate the network performance and provide guidance on the network design while incorporating the effects of traffic unsaturation and interference correlation.

The rest of this paper is organized as follows. The system model and the cooperative scheme under consideration are presented in Section II. In Section III, we derive the stationary interferer density when the network is in a steady state. The correlation of interference power in two consecutive time-slots is characterized in Section IV. In Section V, we analyze the outage probability and average packet delay of the cooperative truncated ARQ scheme. Numerical results are given in Section VI. Finally, Section VII concludes this work.

II. System Model

A. Network and Channel Models

Consider a decentralized wireless ad hoc network with nodes independently and randomly distributed in a two-dimensional coverage area. Over a single-frequency channel, the time is slotted and the time-slot duration is a constant. The spatial locations of source nodes at time-slot $t \in \mathbb{N}_+$ form a homogeneous PPP $\Phi_{\mathrm{S}}(t) = \{s_0(t), s_1(t), \cdots\} \subset \mathbb{R}^2$ with density λ_{S} (average number of nodes per unit area). Each source node (e.g., S_i) associates with a destination node (e.g., D_i), which is located at L meters away in a random direction [7], [8]. The destination nodes are not part of PPP $\Phi_{\mathrm{S}}(t)$. Extension to the scenario with random link length is straightforward [24]. Each source node has a buffer of infinite capacity and the initial queue length is independently and randomly chosen [11], [12], [25]. New packets arrive at each source node according to a geometric arrival process with rate (average number of packets per time-slot) $\Lambda_{\mathrm{T}} < 1$, which represents the probability that a new packet arrive in a time-slot. All packets have equal length (i.e., each transmitted in exactly one time-slot with a constant transmission rate), and are served in a first-in first-out (FIFO) manner.

All other nodes are referred to as relays, and they do not have their own packets to transmit. The spatial locations of relays at time-slot t are modeled by another homogeneous PPP, $\Phi_{\mathrm{R}}(t) = \{r_0(t), r_1(t), \cdots\} \subset \mathbb{R}^2$ with density λ_{R}. The capital letter (e.g., S_i, R_i, and D_i) and lowercase letter (e.g., $s_i(t)$, $r_i(t)$, and $d_i(t)$) represent the node and its location, respectively. According to Slivnyak's theorem [26], the reduced Palm distribution equals to its original distribution and the statistics observed from a PPP is independent of the test location. Hence, we consider a typical source-destination pair in the network with the source and destination nodes located at $s_0 = (L, 0)$ and $d_0 = (0, 0)$, respectively. As the relays are homogeneously available for all source-destination pairs, we focus on analyzing the performance of the typical source-destination pair, which holds for all other source-destination pairs in the network [27].

Consider that the network is interference-limited, where the noise power can be ignored. The channel between any pair of nodes is characterized by both large-scale path loss and small-scale Rayleigh fading. The impact of the channel between any pair of nodes (e.g., S_i and R_i) at time-slot t on the received signal power is denoted as $H_{S_iR_i}(t) \cdot d_{S_iR_i}^{-\alpha}(t)$, where $H_{S_iR_i}(t)$ denotes the random distance-independent fading coefficient with unit mean, $d_{S_iR_i}(t) = \|s_i(t) - r_i(t)\|$ denotes the Euclidean distance between the nodes, and $\alpha > 2$ denotes the path loss exponent. The fading coefficients remain invariant during one time-slot and vary independently at different locations and in different time-slots. All source and relay nodes transmit with the same power, without loss of generality, normalized to one. Each node is equipped with one omni-directional antenna and operates in half-duplex mode.

B. Cooperative Scheme

At the beginning of each time-slot, the source node of each potential source-destination pair[1] is granted access to the medium with probability $p_{\mathrm{m}} > 0$, which is independent of the transmission decisions of all other source nodes and its buffer status. Each source node, being granted access to the medium and having a non-empty buffer, transmits a packet to its intended destination node with rate ν (in bit/s). Due to the broadcast nature of wireless communications, the concurrent transmissions across the network generate interference to each other, leading to possible transmission failures. Specifically, a packet transmitted from source node S_0 is successfully received by destination node D_0 at time-slot t if the instantaneous signal-to-interference ratio (SIR) satisfies

$$\gamma_{S_0D_0}(t) = \frac{H_{S_0D_0}(t) \cdot L^{-\alpha}}{\sum\limits_{x \in \Phi_{\mathrm{I}}(t)} H_{XD_0}(t) \cdot d_{XD_0}^{-\alpha}(t)} \geq \beta \tag{1}$$

where $\Phi_{\mathrm{I}}(t)$ denotes the set of the spatial locations of unintended (active) transmitters at time-slot t, x denotes the location coordinate of unintended transmitter X, the denominator is the aggregate interference power observed by destination node D_0 (i.e., summation of power levels of the signals from all unintended transmitters), and β denotes the threshold required for successful packet receptions. The required reception threshold is defined as $\beta \equiv 2^{\nu/B} - 1$ based on Shannon's formula, where B denotes the channel bandwidth in Hz.

Consider a cooperative truncated ARQ scheme with one-time retransmission. If the destination node correctly decodes a packet, it sends an acknowledgement (ACK) frame. In the subsequent time-slot, $t+1$, the source node is granted access to the medium with probability p_{m} to transmit a new packet. Otherwise, a negative acknowledgement (NACK) frame is broadcasted. The undelivered packet is retransmitted in the subsequent time-slot by either the source node or a selected relay according to the following relay selection scheme. Both the ACK and NACK frames are reported back via an error-free and delay-free control channel.

For each source-destination pair requiring the packet retransmission, a spatially constrained relay selection region[2] is considered, which can be identified via location estimation [31] at each node and coordination signaling. Take the typical source-destination pair as an example. The relay selection region of the typical source-destination pair is centered at $(L - \theta, 0)$ with radius r_{C}. In particular, the distance between source node S_0 and the center of its relay selection region is denoted as θ, while the distance between the center of the relay selection region and destination node D_0 is $L - \theta$. A single-relay decode-and-forward (DF) scheme is considered. Note that the probability of having overlapped constrained relay selection regions is low, as the requirement of providing an acceptable outage probability for each source-destination pair limits the density of source nodes. In case the relay selection regions for different source-destination pairs overlap, a relay in the overlapped regions receives the signal from the source node offering the highest received signal power. The relays within the constrained relay selection region are referred to as potential relays. The potential relays having successfully received the packet from the source node are referred to as qualified relays. Let $\Omega_0(t)$ denote the relay set formed by the qualified relays of the typical source-destination pair at time-slot t. Mathematically, relay set $\Omega_0(t)$ can be expressed as

$$\Omega_0(t) = \{R_i : r_i(t) \in \Phi_{\mathrm{R}}(t) \cap \mathrm{CR}_0, \gamma_{S_0R_i}(t) \geq \beta\} \tag{2}$$

where CR_0 denotes the constrained relay selection region for

[1] A potential source-destination pair refers to the source-destination pair that its source node or selected relay does not retransmit a packet in the current time-slot.

[2] It is preferable to select the best relay from a constrained region due to the following reasons: 1) the relays geographically close to the source and destination nodes (e.g., within a constrained region) are more likely to be reliable [9]; 2) restricting the number of contending relays reduces the implementation complexity and protocol overhead of a relay selection scheme [28], [29]; and 3) a constrained relay selection region is beneficial for the efficiency of spatial frequency reuse [30].

the typical source-destination pair, and $\gamma_{S_0R_i}(t)$ denotes the SIR observed by relay R_i at time-slot t.

Any relay can correctly decode at most one packet in one time-slot by setting $\beta > 1$ [10]. Assuming that, via measuring the NACK frame, each qualified relay has the instantaneous channel state information (CSI) towards the intended destination node. As more than one qualified relay may exist, a back-off scheme[3] can be utilized to select the best relay in a distributed way [32]. The source node is treated equivalently as a qualified relay. At the beginning of time-slot $t+1$, a qualified relay with the best instantaneous channel quality to destination node D_0 is selected as the best relay, denoted as R_{b}^0, where the instantaneous channel quality depends on both the path loss and the random channel fading coefficient. In particular, source node S_0 is selected as the best relay R_{b}^0 when either relay set $\Omega_0(t)$ is empty or source node S_0 has the best channel quality to destination node D_0. Otherwise, a qualified relay in $\Omega_0(t)$ with the best channel quality to destination node D_0 acts as the best relay R_{b}^0. At time-slot $t+1$, the best relay R_{b}^0 retransmits the packet to intended destination node D_0 with rate ν, while all other qualified relays for the typical source-destination pair keep silent. Mathematically, the SIR observed by destination node D_0 at time-slot $t+1$ can be expressed as

$$\begin{aligned}&\gamma_{R_{\mathrm{b}}^0D_0}(t+1)\\&=\max\left\{\max_{R_i\in\Omega_0(t)}\left\{\gamma_{R_iD_0}(t+1)\right\},\gamma_{S_0D_0}(t+1)\right\}\end{aligned}\tag{3}$$

where relay set $\Omega_0(t)$ is defined in (2).

The retransmitted packet is successfully received by the destination node if $\gamma_{R_{\mathrm{b}}^0D_0}(t+1) \geq \beta$. Otherwise, an outage event occurs as both the original transmission and retransmission fail to deliver the packet, i.e., $\gamma_{S_0D_0}(t) < \beta$ and $\gamma_{R_{\mathrm{b}}^0D_0}(t+1) < \beta$. Upon the failure of the packet retransmission, the packet is dropped from the queue, and the source node is granted access to the medium with probability p_{m} to transmit a new packet in the subsequent time-slot, $t+2$.

Fig. 1(a) illustrates the transmission process of each packet. Upon being granted access to the medium, the head-of-line (HOL) departs from the buffer of the source node when either it is correctly decoded by the destination node or it is not correctly decoded by the destination node after one retransmission attempt. After the individual cooperative transmission of one packet, the locations of the source node and its selected relay are changed according to a high mobility random walk model as in [11], [12], [33], [34], which allows for decoupling the interaction among the queues and conducting a tractable performance analysis. The analytical results still provide useful insights on the network performance. Note that the time-slot synchronization among the nodes can be maintained by using GPS [5] or by implementing a distributed synchronization scheme [35] in the nodes. With the mobility model, the displacement theorem [36] can be applied, which results in location independence across the transmission periods of different packets.

From a perspective of the overall network, the cooperative truncated ARQ scheme is enabled by all source-destination pairs, leading to asynchronous concurrent cooperative transmissions over different spatial locations. As shown in Fig. 1(b), the concurrent transmitters at any time-slot include the emerging and retransmitting nodes. An emerging node refers to the node transmitting a new packet in the current time-slot, while a retransmitting node refers to the node retransmitting the packet undelivered in the previous time-slot. Enabling more concurrent transmissions is beneficial for the efficiency of spatial frequency reuse. However, as the concurrent transmissions generate interference to each other, a higher density of unintended transmissions increases the packet retransmission probability, and vice versa. Such a correlation should be considered when deriving the interferer density. On the other hand, the correlation of interferer locations in two consecutive time-slots, due to packet retransmissions, induces the correlation of interference power, which leads to the correlation of successful packet receptions and affects the transmission outage probability. As a result, to evaluate the overall network performance, we characterize the interferer density and interference correlation in Sections III and IV, respectively.

III. Interferer Density

The interferer density determines the average interference power observed by each node and hence the probability of transmission failure. In this section, utilizing the tools from queueing theory and stochastic geometry, we derive the interferer density (i.e., density of unintended transmitters) when the network is in a steady state, in terms of the packet arrival rate, source density, medium access probability, and link length.

In deriving the interferer density, the typical source-destination pair is not included in the following sets. Let $\Phi_{\mathrm{em}}(t)$ and $\Phi_{\mathrm{re}}(t)$ be the sets of the spatial locations of emerging and retransmitting nodes at time-slot t, respectively. As in [25] and [37], $\Phi_{\mathrm{em}}(t)$ and $\Phi_{\mathrm{re}}(t)$ can be approximated as PPPs with densities $\lambda_{\mathrm{em}}(t)$ and $\lambda_{\mathrm{re}}(t)$ respectively, and the accuracy is validated by simulations. As an unintended transmitter is either an emerging node or a retransmitting node, we have $\Phi_{\mathrm{I}}(t) = \Phi_{\mathrm{em}}(t) \cup \Phi_{\mathrm{re}}(t)$ and $\lambda_{\mathrm{I}}(t) = \lambda_{\mathrm{em}}(t) + \lambda_{\mathrm{re}}(t)$, where $\lambda_{\mathrm{I}}(t)$ is the interferer density at time-slot t. When the network is in a steady state, the interferer density is stationary, i.e., $\lambda_{\mathrm{I}}(t) = \lambda_{\mathrm{I}}$. Due to the i.i.d. channel fading coefficients in different time-slots and the stationary interferer density, the retransmission probability (i.e., failure probability of the packets transmitted by emerging nodes) is stationary, denoted as q_{f}. Let μ denote the packet transmission rate of each source-destination pair, which depends on medium access probability p_{m} and retransmission probability q_{f}. The probability that each source node has a non-empty buffer is given by the utilization factor, denoted as $\rho = \Lambda_{\mathrm{T}}/\mu$. The traffic unsaturation affects the probability of having an empty queue and the interferer density, which in turn affects the outage probability of each source-destination pair. Captured by the utilization factor, the traffic unsaturation is considered in the following analysis.

[3] Using a back-off scheme, the best relay obtains the shortest back-off duration and broadcasts a signaling frame when its back-off timer expires. Such a signaling frame contains the MAC address of its intended source node. After decoding the signaling frame, each source node can check the MAC address to find out whether or not this relay is the best relay for itself [29], [32].

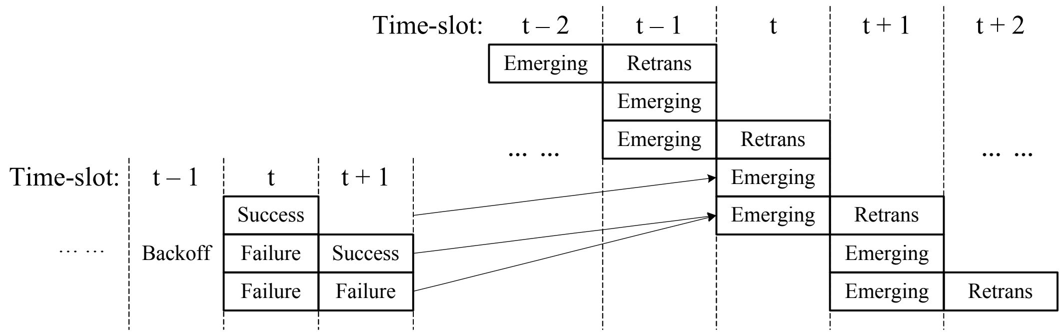

(a) Transmission process of the HOL (b) Concurrent transmissions in the network

Fig. 1: An illustration of the transmission processes of the HOL and all packets in the network, respectively.

At the beginning of time-slot t, the density of source nodes of potential source-destination pairs is $\lambda_{\mathrm{S}} - \lambda_{\mathrm{re}}(t)$. As these source nodes are granted access to the medium with probability p_{m}, the density of emerging nodes at time-slot t is given by $\lambda_{\mathrm{em}}(t) = \rho p_{\mathrm{m}} \left[\lambda_{\mathrm{S}} - \lambda_{\mathrm{re}}(t)\right]$. Because of one-time packet retransmission, the density of retransmitting nodes at time-slot $t+1$ can be expressed as $\lambda_{\mathrm{re}}(t+1) = \lambda_{\mathrm{em}}(t) \cdot q_{\mathrm{f}}$. Hence, the following equation holds

$$\rho p_{\mathrm{m}}[\lambda_{\mathrm{S}} - \lambda_{\mathrm{re}}(t)] \cdot q_{\mathrm{f}} = \lambda_{\mathrm{re}}(t+1) \tag{4}$$

where $\lambda_{\mathrm{re}}(t) = \lambda_{\mathrm{re}}(t+1) = \lambda_{\mathrm{re}}$ when the network is in a steady state.

The time index is dropped whenever the quantities remain invariant over time. According to (4), the densities of retransmitting and emerging nodes at any time-slot can be expressed respectively as

$$\begin{aligned} \lambda_{\mathrm{re}} &= \frac{q_{\mathrm{f}}}{1+\rho p_{\mathrm{m}} q_{\mathrm{f}}} \rho p_{\mathrm{m}} \lambda_{\mathrm{S}} \\ \lambda_{\mathrm{em}} &= \frac{1}{1+\rho p_{\mathrm{m}} q_{\mathrm{f}}} \rho p_{\mathrm{m}} \lambda_{\mathrm{S}}. \end{aligned} \tag{5}$$

As a result, the stationary interferer density is given by

$$\lambda_{\mathrm{I}} = \lambda_{\mathrm{em}} + \lambda_{\mathrm{re}} = \frac{1+q_{\mathrm{f}}}{1+\rho p_{\mathrm{m}} q_{\mathrm{f}}} \rho p_{\mathrm{m}} \lambda_{\mathrm{S}}. \tag{6}$$

The utilization factor ρ and retransmission probability q_{f} are derived in the following two propositions.

Proposition 1. *Given that all source nodes have stable queues and the network is in a steady state, the utilization factor of each source node is given by*

$$\rho = \Lambda_{\mathrm{T}}(1 + p_{\mathrm{m}} q_{\mathrm{f}})/p_{\mathrm{m}}. \tag{7}$$

Proof: See Appendix A. ■

After obtaining utilization factor ρ, we derive retransmission probability q_{f} and stationary interferer density λ_{I} in the following proposition.

Proposition 2. *Given that all source nodes have stable queues and the network is in a steady state, the stationary interferer density is given by*

$$\lambda_{\mathrm{I}} = \Lambda_{\mathrm{T}} \lambda_{\mathrm{S}} \cdot g\left(q_{\mathrm{f}}\right) \tag{8}$$

where q_{f} is a unique solution of the following fixed-point equation

$$q_{\mathrm{f}} = 1 - \exp\left[-\Lambda_{\mathrm{T}} \lambda_{\mathrm{S}} C_1 \cdot g\left(q_{\mathrm{f}}\right)\right] \tag{9}$$

with $\delta = 2/\alpha$, and

$$C_1 = \frac{\pi^2 \delta}{\sin\left(\pi\delta\right)} \beta^{\delta} L^2 \tag{10}$$

$$g\left(q_{\mathrm{f}}\right) = \frac{\left(1+q_{\mathrm{f}}\right)\left(1+p_{\mathrm{m}} q_{\mathrm{f}}\right)}{1+\Lambda_{\mathrm{T}}\left(1+p_{\mathrm{m}} q_{\mathrm{f}}\right) q_{\mathrm{f}}}. \tag{11}$$

Proof: See Appendix B. ■

The retransmission probability q_{f} can be easily calculated by solving a fixed-point equation in (9). Eqs. (8) and (9) capture the correlation between stationary interferer density λ_{I} and retransmission probability q_{f}.

Propositions 1 and 2 present utilization factor ρ, interferer density λ_{I}, and retransmission probability q_{f} under the condition that the network is stable. In the following corollary, we provide a sufficient condition for the network stability.

Corollary 1. *A sufficient condition for the queues of all source nodes to be stable is given by*

$$\Lambda_{\mathrm{T}} < p_{\mathrm{m}}/(1 + p_{\mathrm{m}} q_{\mathrm{f}}) \tag{12}$$

where q_{f} is a unique solution of the following fixed-point equation

$$q_{\mathrm{f}} = 1 - \exp\left(-\frac{\left(1+q_{\mathrm{f}}\right) p_{\mathrm{m}}}{1+p_{\mathrm{m}} q_{\mathrm{f}}} \lambda_{\mathrm{S}} C_1\right). \tag{13}$$

Proof: See Appendix C. ■

IV. Interference Correlation

The transmission of one packet lasts for two time-slots when a retransmission is required. For each source-destination pair requiring a packet retransmission, the locations of transmitting and retransmitting nodes are correlated. Due to concurrent packet retransmissions, the interference power correlates in two consecutive time-slots. In this section, we characterize and distinguish the interference correlation incurred by (interfering) source and relay retransmissions by deriving their respective densities.

At time-slot $t+1$, the set of retransmitting nodes, $\Phi_{\mathrm{re}}\left(t+1\right)$, can be further partitioned into two independent

PPPs, $\Phi_{\text{reS}}(t+1)$ and $\Phi_{\text{reR}}(t+1)$. Mathematically, we have

$$\Phi_{\text{re}}(t+1) = \Phi_{\text{reS}}(t+1) \cup \Phi_{\text{reR}}(t+1) \tag{14}$$

where $\Phi_{\text{reS}}(t+1)$ and $\Phi_{\text{reR}}(t+1)$ denote the sets of the geographical locations of retransmitting sources and relays at time-slot $t+1$, respectively.

The sets of the locations of retransmitting source and relay nodes can be expressed respectively as

$$\begin{aligned}&\Phi_{\text{reS}}(t+1)\\ &= \{s_i(t+1) \in \Phi_{\text{re}}(t+1) : s_i(t+1) = s_i(t)\}\end{aligned} \tag{15}$$

and

$$\begin{aligned}&\Phi_{\text{reR}}(t+1)\\ &= \{r_i(t+1) \in \Phi_{\text{re}}(t+1) : r_i(t+1) = s_i(t) + \tau\}\end{aligned} \tag{16}$$

where $s_i(t) \in \Phi_{\text{em}}(t)$ and τ is the location difference between a source and the selected relay.

At any time-slot t, the relays within constrained relay selection region CR_0 and destination node D_0 locate geographically close and suffer from the same set of interferers $\Phi_{\text{I}}(t)$, yielding to the spatial correlation of interference power observed by these nodes. On the other hand, the common locations of transmitting and retransmitting sources, $\Phi_{\text{reS}}(t+1)$ defined in (15), and the adjacent locations of transmitting sources and retransmitting relays, $\Phi_{\text{reR}}(t+1)$ defined in (16), yield to the temporal correlation of interference power observed by destination node D_0 in consecutive time-slots t and $t+1$. The temporal interference correlation is characterized by the densities of retransmitting sources and relays, denoted as λ_{reS} and λ_{reR} respectively, which are derived based on the relay selection scheme. The effect of interference correlation on the network performance is considered in the following analysis.

According to the relay selection scheme, source node S_0 retransmits the packet at time-slot $t+1$ when one of the following events occurs: 1) Event $\mathcal{E}_{11}$ - destination node D_0 fails to decode the packet at time-slot t, and relay set $\Omega_0(t)$ is empty; 2) Event $\mathcal{E}_{12}$ - destination node D_0 fails to decode the packet at time-slot t, and source node S_0 has the best channel to destination node D_0 while relay set $\Omega_0(t)$ is not empty. The probability of Event $\mathcal{E}_{11}$ can be expressed as

$$\begin{aligned}&\mathbb{P}(\mathcal{E}_{11}) = \mathbb{P}(\gamma_{S_0D_0}(t) < \beta, \Omega_0(t) = \emptyset)\\ &\overset{(a)}{=} \sum_{k=0}^{\infty} \mathbb{P}(K_0 = k) \cdot \mathbb{P}(\gamma_{S_0D_0}(t) < \beta, M_0 = 0 \,|K_0 = k)\end{aligned} \tag{17}$$

where K_0 and M_0 denote the numbers of potential and qualified relays respectively, $\mathbb{P}(K_0 = k) = \left(\lambda_{\text{R}}\pi r_{\text{C}}^2\right)^k \exp\left(-\lambda_{\text{R}}\pi r_{\text{C}}^2\right)\Big/k!$, and (a) follows by conditioning on the value of K_0.

Denote Event $\mathcal{E}_{13}$ as the event that source node S_0 has the best channel to destination node D_0. By definition, the probability of Event $\mathcal{E}_{12}$ is given by

$$\begin{aligned}&\mathbb{P}(\mathcal{E}_{12}) = \mathbb{P}(\gamma_{S_0D_0}(t) < \beta, \Omega_0(t) \neq \emptyset, \mathcal{E}_{13})\\ &\overset{(a)}{=} \sum_{k=1}^{\infty} \mathbb{P}(K_0 = k)\\ &\times \left[\sum_{m=1}^{k} \mathbb{P}(\gamma_{S_0D_0}(t) < \beta, M_0 = m, \mathcal{E}_{13}(m) \,|K_0 = k)\right]\end{aligned} \tag{18}$$

where (a) follows by conditioning on the value of K_0, and $\mathcal{E}_{13}(m)$ denotes the event that $\mathcal{E}_{13}$ happens when there are m qualified relays.

The probability that destination node D_0 fails to decode the packet while there exist m qualified relays (i.e., $k-m$ potential relays fail to decode the packet) is given by (19), shown at the top of the next page, where $I_{D_0}(t) = \sum\limits_{x\in\Phi_{\text{I}}(t)} H_{XD_0}(t)\, d_{XD_0}^{-\alpha}(t)$ and $I_{R_i}(t) = \sum\limits_{x\in\Phi_{\text{I}}(t)} H_{XR_i}(t)\, d_{XR_i}^{-\alpha}(t)$ denote the aggregate interference power observed by destination node D_0 and relay R_i at time-slot t respectively, (a) follows by taking expectations over independent channel fading coefficients $H_{S_0D_0}(t)$ and $H_{S_0R_i}(t)$, by setting the distances between source node S_0 and its potential relays to be θ for small constrained relay selection regions, and by applying the independent channel fading in different time-slots and for different channels. Note that the spatial interference correlation is taken into account by taking a joint expectation over the same set of interferers $\Phi_{\text{I}}(t)$.

Similarly, by taking the Laplace transforms of independent channel fading coefficients $H_{XD_0}(t)$ and $H_{XR_i}(t)$, we have

$$\begin{aligned}\mathcal{P} = \mathbb{E}_{\Phi_{\text{I}}(t)}\Bigg[&\binom{k}{m}\left(1 - \prod_{x\in\Phi_{\text{I}}(t)} \eta_{11}\right)\left(\prod_{x\in\Phi_{\text{I}}(t)} \eta_{22}\right)^m\\ &\times \left(1 - \prod_{x\in\Phi_{\text{I}}(t)} \eta_{22}\right)^{k-m}\Bigg]\end{aligned} \tag{20}$$

where $\eta_{jl} = \left(1 + \beta u_j^{\alpha} v_l^{-\alpha}\right)^{-1}$. Note that $u_j \in \{L, \theta, L-\theta\}$ and $v_l \in \{d_{XD_0}(t), d_{XR_0}(t)\}$, where $d_{XD_0}(t) = \|x\|$ and $d_{XR_0}(t) = \|x - r_0\|$.

By applying the binomial expansion in (20), we obtain (21), shown at the top of the next page, where (a) follows from the probability generating functional (PGFL) of the PPP [3], $\Gamma(x)$ is the Gamma function, and

$$Q_{m+n} = -\delta\pi\beta^{\delta}\theta^2\Gamma(-\delta)\,\Gamma(\delta+m+n)\big/\Gamma(m+n). \tag{22}$$

By setting $m = 0$ and substituting (21) into (17), we obtain $\mathbb{P}(\mathcal{E}_{11})$.

Given that there are m qualified relays, the probability that source node S_0 has the best channel to destination node D_0

$$\begin{aligned}
&\mathbb{P}\left(\gamma_{S_0D_0}\left(t\right)<\beta, M_0=m, \mathcal{E}_{13}(m)\left|K_0=k\right.\right)\\
&\overset{(a)}{=}\mathbb{E}_{\Phi_{\mathrm{I}}(t),H}\left[\left[1-\exp\left(-\beta L^{\alpha} I_{D_0}\left(t\right)\right)\right]\binom{k}{m}\prod_{i=1}^{m}\exp\left(-\beta\theta^{\alpha} I_{R_i}\left(t\right)\right)\prod_{j=1}^{k-m}\left[1-\exp\left(-\beta\theta^{\alpha} I_{R_j}\left(t\right)\right)\right]\right]\cdot\mathbb{P}\left(\mathcal{E}_{13}(m)\right)\\
&=\mathcal{P}\cdot\mathbb{P}\left(\mathcal{E}_{13}(m)\right)
\end{aligned}\tag{19}$$

$$\begin{aligned}
\mathcal{P}=&\binom{k}{m}\sum_{n=0}^{k-m}\binom{k-m}{n}(-1)^n\left\{\mathbb{E}_{\Phi_{\mathrm{I}}(t)}\left[\prod_{x\in\Phi_{\mathrm{I}}(t)}\eta_{22}^{m+n}\right]-\mathbb{E}_{\Phi_{\mathrm{I}}(t)}\left[\prod_{x\in\Phi_{\mathrm{I}}(t)}\eta_{11}\eta_{22}^{m+n}\right]\right\}\\
\overset{(a)}{=}&\binom{k}{m}\sum_{n=0}^{k-m}\binom{k-m}{n}(-1)^n\left\{\exp\left(-\lambda_{\mathrm{I}}Q_{m+n}\right)-\exp\left[-\lambda_{\mathrm{I}}\int_{\mathbb{R}^2}\left(1-\eta_{11}\eta_{22}^{m+n}\right)\mathrm{d}x\right]\right\}
\end{aligned}\tag{21}$$

---

is given by

$$\begin{aligned}
&\mathbb{P}\left(\mathcal{E}_{13}(m)\right)\\
=&\mathbb{P}\left(H_{S_0D_0}\left(t+1\right)>\left(\frac{L}{L-\theta}\right)^{\alpha}\max_{R_i\in\Omega_0(t)}\left\{H_{R_iD_0}\left(t+1\right)\right\}\right)\\
=&\prod_{i=1}^{m}\mathbb{P}\left(H_{S_0D_0}\left(t+1\right)>\left(\frac{L}{L-\theta}\right)^{\alpha}H_{R_iD_0}\left(t+1\right)\right)\\
=&\left[1+\left(\frac{L}{L-\theta}\right)^{\alpha}\right]^{-m}.
\end{aligned}\tag{23}$$

Substituting (21) and (23) into (18), we obtain $\mathbb{P}\left(\mathcal{E}_{12}\right)$. With $\mathbb{P}\left(\mathcal{E}_{11}\right)$ and $\mathbb{P}\left(\mathcal{E}_{12}\right)$, the probability of the source node retransmitting, denoted as q_{s}, is given by $q_{\mathrm{s}}=\mathbb{P}\left(\mathcal{E}_{11}\right)+\mathbb{P}\left(\mathcal{E}_{12}\right)$. As a result, the densities of retransmitting sources and relays are given by

$$\begin{aligned}
\lambda_{\mathrm{reS}}&=q_{\mathrm{s}}\lambda_{\mathrm{re}}/q_{\mathrm{f}}\\
\lambda_{\mathrm{reR}}&=\left(q_{\mathrm{f}}-q_{\mathrm{s}}\right)\lambda_{\mathrm{re}}/q_{\mathrm{f}}
\end{aligned}\tag{24}$$

where λ_{re} and q_{f} are defined in (5) and (9), respectively.

V. Performance Analysis

After deriving the stationary interferer density in Section III and characterizing the interference correlation in two consecutive time-slots in Section IV, we derive the outage probability and average delay in terms of important network and protocol parameters in this section.

For performance comparison, we first consider a conventional truncated ARQ scheme, where only the source nodes retransmit the packets upon the transmission failure. An outage event occurs when the received SIRs at the destination node (e.g., D_0) are smaller than reception threshold β in two consecutive time-slots. The outage probability, denoted as $q_{\mathrm{out}}^{\mathrm{Conv}}$, is given in the following proposition.

Proposition 3. *The outage probability of the conventional truncated ARQ scheme is given by*

$$\begin{aligned}
q_{\mathrm{out}}^{\mathrm{Conv}}=&1-2\exp\left(-\lambda_{\mathrm{I}}C_1\right)\\
&+\left[\exp\left(-\lambda_{\mathrm{em}}C_1\right)\right]^2\exp\left(-\lambda_{\mathrm{re}}C_2\right)
\end{aligned}\tag{25}$$

where C_1 is defined in (10), and

$$C_2=\pi\beta^{\delta}\Gamma\left(1+\delta\right)\Gamma\left(1-\delta\right)\left(1+\delta\right)L^2.\tag{26}$$

Proof: See Appendix D. ∎

For a cooperative truncated ARQ scheme, an outage event occurs when both of the following events occur: 1) Event $\mathcal{E}_{21}$ - the direct link is not reliable in both time-slots t and $t+1$; 2) Event $\mathcal{E}_{22}$ - no relays have reliable links to the source and destination nodes in time-slots t and $t+1$, respectively. The outage probability, denoted as $q_{\mathrm{out}}^{\mathrm{Coop}}$, is given in the following proposition.

Proposition 4. *The outage probability of the cooperative truncated ARQ scheme is given by*

$$q_{\mathrm{out}}^{\mathrm{Coop}}=\sum_{k=0}^{\infty}\frac{\left(\lambda_{\mathrm{R}}\pi r_{\mathrm{C}}^2\right)^k}{k!}\exp\left(-\lambda_{\mathrm{R}}\pi r_{\mathrm{C}}^2\right)\sum_{m=0}^{k}\binom{k}{m}(-1)^m C_3\tag{27}$$

where C_3 is given in (28) with λ_{em}, λ_{reS}, λ_{reR}, and Q_m are defined in (5), (24), and (22) respectively, $T_m=Q_m(L-\theta)^2\big/\theta^2$, $C_{31}=\int_{\mathbb{R}^2}(1-\eta_{11}\eta_{22}^m)\mathrm{d}x$, and $C_{32}=\int_{\mathbb{R}^2}(1-\eta_{11}\eta_{31}^m)\mathrm{d}x$.

Proof: See Appendix E. ∎

The average delay is composed of queueing delay and service delay. Queueing delay is the duration between the time that a packet arrives at the queue and the time that it becomes the HOL. Service delay is the duration between the time that a packet becomes the HOL until it leaves the queue. According to the service time distribution in (33) derived in Appendix A, the second moment of the service time is given by

$$\begin{aligned}
&\mathbb{E}\left[U^2\right]=p_{\mathrm{m}}\left(1-q_{\mathrm{f}}\right)\\
&+\sum_{k=2}^{\infty}k^2\left[\left(1-p_{\mathrm{m}}\right)^{k-1}p_{\mathrm{m}}\left(1-q_{\mathrm{f}}\right)+\left(1-p_{\mathrm{m}}\right)^{k-2}p_{\mathrm{m}}q_{\mathrm{f}}\right]\\
&=\left(2-p_{\mathrm{m}}+2p_{\mathrm{m}}q_{\mathrm{f}}+p_{\mathrm{m}}^2q_{\mathrm{f}}\right)\big/p_{\mathrm{m}}^2.
\end{aligned}\tag{29}$$

The queueing delay of a Geo/G/1 queue [38], denoted as W_{q}, is given by

$$W_{\mathrm{q}}=\frac{\Lambda_{\mathrm{T}}(\mathbb{E}\left[U^2\right]-\mathbb{E}\left[U\right])}{2\left(1-\Lambda_{\mathrm{T}}\mathbb{E}\left[U\right]\right)}\tag{30}$$

$$
\begin{aligned}
C_3 = &\exp\left(-\lambda_{\text{em}}(Q_m + T_m) - \lambda_{\text{reS}}\int_{\mathbb{R}^2}(1-\eta_{22}^m\eta_{31}^m)\,\mathrm{d}x - \lambda_{\text{reR}}\int_{\mathbb{R}^2}(1-\eta_{21}^m\eta_{31}^m)\,\mathrm{d}x\right)\\
&- \exp\left(-\lambda_{\text{em}}(T_m + C_{31}) - \lambda_{\text{reS}}\int_{\mathbb{R}^2}(1-\eta_{11}\eta_{22}^m\eta_{31}^m)\,\mathrm{d}x - \lambda_{\text{reR}}\int_{\mathbb{R}^2}(1-\eta_{11}\eta_{21}^m\eta_{31}^m)\,\mathrm{d}x\right)\\
&- \exp\left(-\lambda_{\text{em}}(Q_m + C_{32}) - \lambda_{\text{reS}}\int_{\mathbb{R}^2}(1-\eta_{11}\eta_{22}^m\eta_{31}^m)\,\mathrm{d}x - \lambda_{\text{reR}}\int_{\mathbb{R}^2}(1-\eta_{11}\eta_{21}^m\eta_{31}^m)\,\mathrm{d}x\right)\\
&+ \exp\left(-\lambda_{\text{em}}(C_{31} + C_{32}) - \lambda_{\text{reS}}\int_{\mathbb{R}^2}(1-\eta_{11}^2\eta_{22}^m\eta_{31}^m)\,\mathrm{d}x - \lambda_{\text{reR}}\int_{\mathbb{R}^2}(1-\eta_{11}^2\eta_{21}^m\eta_{31}^m)\,\mathrm{d}x\right)
\end{aligned} \tag{28}
$$

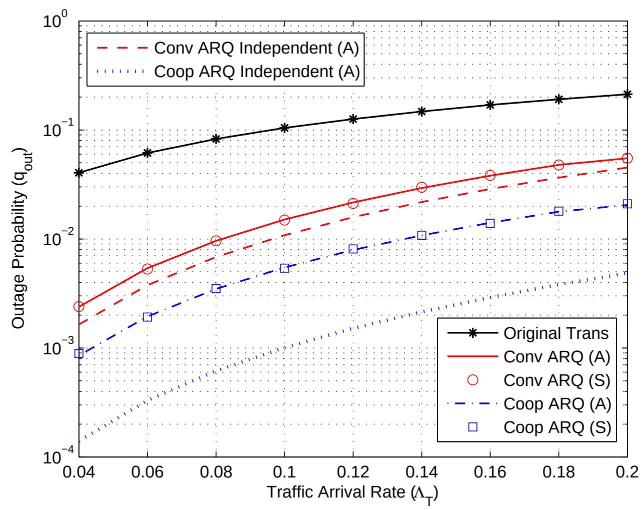

Fig. 2: Outage probability versus traffic arrival rate (in packets/time-slot) when $\lambda_S = 0.001$ nodes/m^2, $\lambda_R = 0.2$ nodes/m^2, $p_m = 0.2$, $\theta = 5$ m, and $L = 10$ m.

where $\mathbb{E}[U]$ is provided in (34).

The service delay of a successful packet transmission is given by

$$W_s = \left[1 + \left(q_f - q_{\text{out}}^{\text{Coop}}\right)p_m\right]/p_m \tag{31}$$

where q_f and $q_{\text{out}}^{\text{Coop}}$ are given in (9) and (27), respectively.

As a result, by combining (30) and (31), we can obtain the average delay of a successful packet transmission by

$$W = W_q + W_s. \tag{32}$$

VI. Numerical Results

This section presents both analytical (A) and simulation (S) results for conventional and cooperative truncated ARQ schemes in a decentralized wireless network. In the simulations, a circular network coverage area with radius 1000 m is considered. The reception threshold β and radius of relay selection region r_C are set to 4 and 2 respectively, with path loss exponent $\alpha = 4$. As the performance of the cooperative truncated ARQ scheme is determined by the channel qualities of both the source-relay and relay-destination links, we set the center of the relay selection region at the link center, i.e., $\theta = L/2$. The simulation results are obtained by averaging 10^6 realizations of the random network topology.

Fig. 2 shows the outage probabilities of both conventional and cooperative truncated ARQ schemes versus traffic arrival rate Λ_T with parameters $\lambda_S = 0.001$ nodes/m^2, $\lambda_R = 0.2$ nodes/m^2, $p_m = 0.2$, $\theta = 5$ m, and $L = 10$ m, where the analytical results are obtained based on (25) and (27), respectively. To illustrate the impact of interference correlation, the analytical results of outage probabilities of both schemes under the assumption that the interference power is independent at adjacent locations and in consecutive time-slots are also plotted in Fig. 2. It is shown that the outage probability incorporating the effect of interference correlation is always higher than that assuming independent interference power, as the correlated interference power reduces the benefit achieved by packet retransmissions. The simulation results match well with the analytical results incorporating the effect of interference correlation, which validates the performance analysis. In addition, it is observed that the outage probabilities of both schemes increase with the traffic arrival rate. With an increase of the traffic arrival rate, the probability of having an empty queue at a source node decreases, which leads to a higher density of concurrent transmitters as well as higher interference power observed by a receiver. Compared to the failure probability of the original transmission, both schemes enhance the transmission reliability. By exploiting the spatial diversity gain, the outage probability of the cooperative truncated ARQ scheme is always lower than that of the conventional truncated ARQ scheme.

Fig. 3 illustrates the average delay of the cooperative truncated ARQ scheme versus traffic arrival rate Λ_T for medium access probability $p_m = 0.1$, 0.15, and 0.2 when $\lambda_S = 0.001$ nodes/m^2, $\lambda_R = 0.2$ nodes/m^2, $\theta = 5$ m, and $L = 10$ m, where the analytical result is obtained based on (32). It is observed that the average delay increases significantly with the traffic arrival rate. With an increase of the traffic arrival rate, the queueing delay becomes a more dominant component of the total delay and approaches to infinity when utilization factor ρ tends to 1. On the other hand, with an increase of medium access probability p_m, the packet transmission rate of each source-destination pair increases, which in turn decreases the average delay.

Fig. 4 shows the outage probabilities of both conventional and cooperative truncated ARQ schemes versus medium access probability p_m with parameters $\lambda_S = 0.002$ nodes/m^2, $\lambda_R = 0.2$ nodes/m^2, $\Lambda_T = 0.08$ packets/time-slot, $\theta = 5$ m, and $L = 10$ m. With an increase of the medium access probability, the outage probabilities of both schemes increase

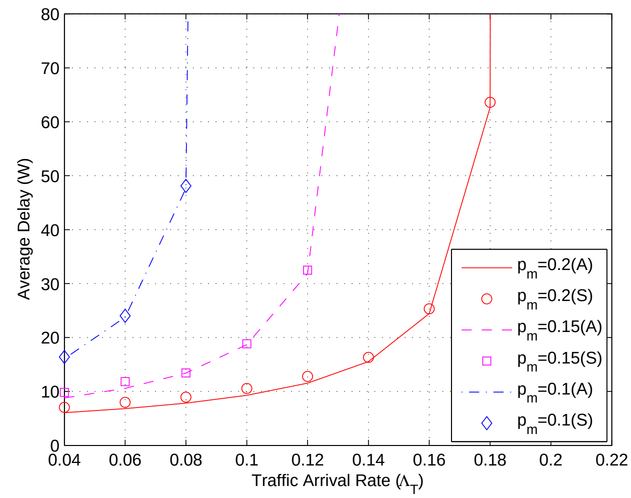

Fig. 3: Average delay versus traffic arrival rate (in packets/time-slot) when $\lambda_{\rm S} = 0.001$ nodes/m^2, $\lambda_{\rm R} = 0.2$ nodes/m^2, $\theta = 5$ m, and $L = 10$ m.

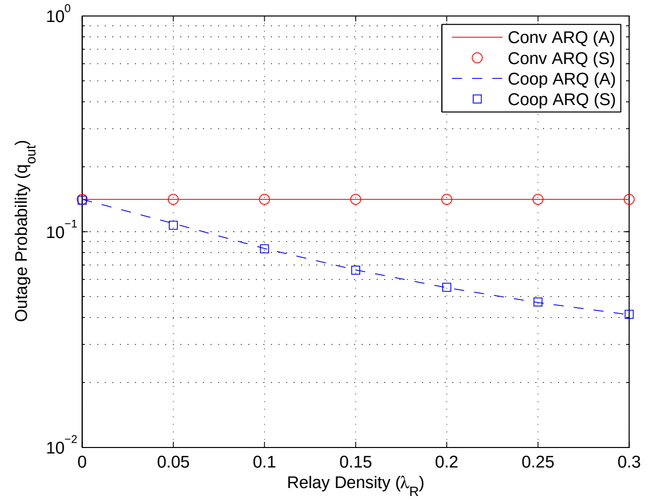

Fig. 5: Outage probability versus relay density when $\lambda_{\rm S} = 0.0015$ nodes/m^2, $\Lambda_{\rm T} = 0.2$ packets/time-slot, $p_{\rm m} = 0.4$, $\theta = 5$ m, and $L = 10$ m.

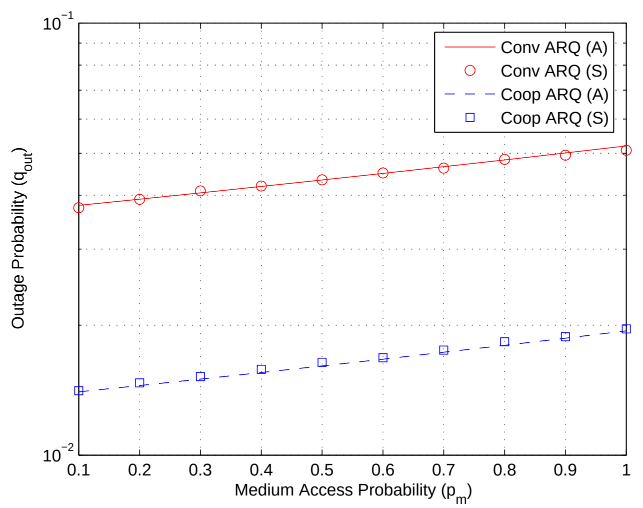

Fig. 4: Outage probability versus medium access probability when $\lambda_{\rm S} = 0.002$ nodes/m^2, $\lambda_{\rm R} = 0.2$ nodes/m^2, $\Lambda_{\rm T} = 0.08$ packets/time-slot, $\theta = 5$ m, and $L = 10$ m.

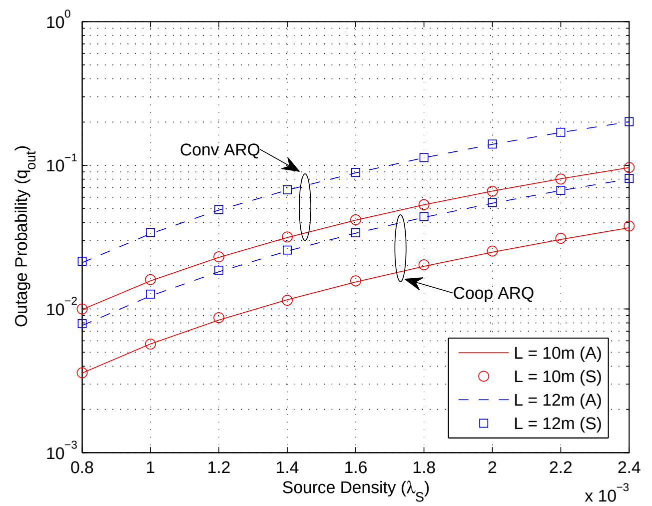

Fig. 6: Outage probability versus source density and link length when $\lambda_{\rm R} = 0.2$ nodes/m^2, $\Lambda_{\rm T} = 0.1$ packets/time-slot, $\theta = L/2$, and $p_{\rm m} = 0.4$.

due to a higher interferer density at each time-slot. Comparing the results in Figs. 2 and 4, it is observed that the impact of medium access probability $p_{\rm m}$ on the outage probability is smaller than the impact of traffic arrival rate $\Lambda_{\rm T}$ on the outage probability. This is due to the fact that, with an increase of medium access probability $p_{\rm m}$, the probability of having an empty queue at each source node decreases, which in turn reduces the interferer density. As a result, combining these two conflict effects on the interferer density, the outage probabilities increase slowly with the medium access probability. On the other hand, comparing the results in Figs. 3 and 4, the average delay decreases with the medium access probability while the outage probability increases with the medium access probability. This implies that the medium access probability can be adjusted to balance the tradeoff between the average delay and outage probability.

Fig. 5 illustrates the outage probabilities of both conventional and cooperative truncated ARQ schemes versus relay density $\lambda_{\rm R}$ with parameters $\lambda_{\rm S} = 0.0015$ nodes/m^2, $p_{\rm m} = 0.4$, $\theta = 5$ m, $\Lambda_{\rm T} = 0.2$ packets/time-slot, and $L = 10$ m. It is observed that the outage probability of the cooperative truncated ARQ scheme decreases with the relay density, while that of the conventional truncated ARQ scheme does not change. With an increase of the relay density, more potential relays are available, which results in a higher probability of selecting a reliable relay. The outage probability of the cooperative truncated ARQ scheme is always lower than that of the conventional truncated ARQ scheme, as the node (i.e., a source node or qualified relay) with the best channel quality to the destination node is selected to retransmit the packet.

Fig. 6 shows the outage probabilities of both conventional and cooperative truncated ARQ schemes versus source density $\lambda_{\rm S}$ and link length L with parameters $\lambda_{\rm R} = 0.2$ nodes/m^2, $\Lambda_{\rm T} = 0.1$ packets/time-slot, $\theta = L/2$, and $p_{\rm m} = 0.4$. With an increase of the source density, the outage probabilities of both schemes increase, because activating more concurrent transmissions leads to higher interference power observed by a destination node. On the other hand, the outage probabilities of both schemes increases with the link length due to a larger path loss between the source and destination nodes.

VII. Conclusions

In this paper, we study the performance of a cooperative truncated ARQ scheme in a decentralized wireless network under unsaturated traffic conditions with randomly positioned single-hop source-destination pairs and relays, where the interference power is spatially and temporally correlated. To evaluate the network performance, we characterize the interference power by deriving the stationary interferer density and identifying the interference correlation in two consecutive time-slots, utilizing the tools from queueing theory and stochastic geometry. The outage probability and average packet delay of the cooperative truncated ARQ scheme are derived as a function of important network and protocol parameters. Extensive simulations are conducted to validate the performance analysis. The analytical results show that the performance analysis under the assumption of independent interference power overestimates the network performance. Further studies include extending the theoretical performance analysis framework presented here to evaluate the performance of cooperative communication in decentralized multi-hop ad hoc networks.

Appendix

A. Proof of Proposition 1

Let U denote the number of time-slots required to transmit the HOL. Starting from time-slot 1, u time-slots are required if 1) the source node is granted access to the medium and transmits the HOL successfully at the uth time-slot; 2) the source node is granted access to the medium at the $(u-1)$th time-slot and retransmits the HOL at the uth time-slot. As the packet arrivals follow a geometric distribution, the queue of each source node can be modeled by a Geo/G/1 queue and its service time distribution is given by

$$\begin{aligned}\mathbb{P}(U=1) &= p_{\mathrm{m}}(1-q_{\mathrm{f}}), && u=1\\ \mathbb{P}(U=u) &= (1-p_{\mathrm{m}})^{u-1}p_{\mathrm{m}}(1-q_{\mathrm{f}}) \\ &\quad + (1-p_{\mathrm{m}})^{u-2}p_{\mathrm{m}}q_{\mathrm{f}}, && u\geq 2.\end{aligned} \tag{33}$$

Hence, the expectation of the service time is given by

$$\mathbb{E}[U] = \sum_{u=1}^{\infty} u\cdot\mathbb{P}(U=u) = (1+p_{\mathrm{m}}q_{\mathrm{f}})/p_{\mathrm{m}}. \tag{34}$$

By definition, the utilization factor is

$$\rho = \Lambda_{\mathrm{T}}/\mu = \Lambda_{\mathrm{T}}\mathbb{E}[U] = \Lambda_{\mathrm{T}}(1+p_{\mathrm{m}}q_{\mathrm{f}})/p_{\mathrm{m}}. \tag{35}$$

B. Proof of Proposition 2

By substituting (7) into (6), we obtain interferer density λ_{I} as a function of retransmission probability q_{f}, as shown in (8). The next step is to derive retransmission probability q_{f} and prove its uniqueness. The original transmission fails when the SIR observed by the destination node (e.g., D_0) is smaller than the required reception threshold. The retransmission probability is given by

$$\begin{aligned}q_{\mathrm{f}} &= \mathbb{P}\left(\gamma_{S_0D_0}(t)<\beta\right)\\ &\overset{(a)}{=} 1-\exp\left(-\lambda_{\mathrm{I}}C_1\right)\\ &\overset{(b)}{=} 1-\exp\left[-\Lambda_{\mathrm{T}}\lambda_{\mathrm{S}}C_1\cdot g(q_{\mathrm{f}})\right]\end{aligned} \tag{36}$$

where C_1 and $g(q_{\mathrm{f}})$ are defined in (10) and (11) respectively, (a) follows from the results presented in [36], and (b) follows by substituting (8).

Let $\Delta(q_{\mathrm{f}})$ denote the right hand side of fixed-point equation (36). As $0<\Delta(0)<\Delta(1)<1$ and $0\leq q_{\mathrm{f}}\leq 1$, there exists at least one solution. In order to prove that (36) has a unique solution, based on Contraction Mapping Theorem [39], we need to show that the first derivative of $\Delta(q_{\mathrm{f}})$ with respect to q_{f} is smaller than one. As a result, we need to show that

$$\Delta'(q_{\mathrm{f}}) = \exp\left[-\Lambda_{\mathrm{T}}\lambda_{\mathrm{S}}C_1\cdot g(q_{\mathrm{f}})\right]\cdot\Lambda_{\mathrm{T}}\lambda_{\mathrm{S}}C_1\cdot g'(q_{\mathrm{f}}) < 1 \tag{37}$$

where $\Delta'(q_{\mathrm{f}})$ and $g'(q_{\mathrm{f}})$ are the first derivatives of $\Delta(q_{\mathrm{f}})$ and $g(q_{\mathrm{f}})$, respectively.

Equivalently, we need to prove that

$$\Psi(q_{\mathrm{f}}) = \exp\left[\Lambda_{\mathrm{T}}\lambda_{\mathrm{S}}C_1\cdot g(q_{\mathrm{f}})\right] - \Lambda_{\mathrm{T}}\lambda_{\mathrm{S}}C_1\cdot g'(q_{\mathrm{f}}) > 0. \tag{38}$$

The above inequality holds if 1) $\Psi(q_{\mathrm{f}})$ is an increasing function of q_{f}; and 2)

$$\exp\left[\Lambda_{\mathrm{T}}\lambda_{\mathrm{S}}C_1\cdot g(0)\right] > \Lambda_{\mathrm{T}}\lambda_{\mathrm{S}}C_1\cdot g'(0). \tag{39}$$

In order to show that $\Psi(q_{\mathrm{f}})$ is an increasing function of q_{f}, we need to prove that the first derivative $\Psi'(q_{\mathrm{f}})$ is larger than 0. The first derivative is given by

$$\begin{aligned}\Psi'(q_{\mathrm{f}}) =& \exp\left[\Lambda_{\mathrm{T}}\lambda_{\mathrm{S}}C_1\cdot g(q_{\mathrm{f}})\right]\cdot\Lambda_{\mathrm{T}}\lambda_{\mathrm{S}}C_1\cdot g'(q_{\mathrm{f}})\\ &-\Lambda_{\mathrm{T}}\lambda_{\mathrm{S}}C_1\cdot g''(q_{\mathrm{f}})\end{aligned} \tag{40}$$

where $g''(q_{\mathrm{f}})$ is the second derivative of $g(q_{\mathrm{f}})$, and

$$g'(q_{\mathrm{f}}) = \frac{-\Lambda_{\mathrm{T}}p_{\mathrm{m}}^2q_{\mathrm{f}}^2 + 2p_{\mathrm{m}}(1-\Lambda_{\mathrm{T}})q_{\mathrm{f}} + 1 + p_{\mathrm{m}} - \Lambda_{\mathrm{T}}}{\left[1+\Lambda_{\mathrm{T}}(1+p_{\mathrm{m}}q_{\mathrm{f}})q_{\mathrm{f}}\right]^2}. \tag{41}$$

Knowing that $0<\Lambda_{\mathrm{T}}<p_{\mathrm{m}}\leq 1$ and $0\leq q_{\mathrm{f}}\leq 1$, we have $g'(q_{\mathrm{f}})>0$. As all parameters are larger than or equal to 0, we have $\exp\left[\Lambda_{\mathrm{T}}\lambda_{\mathrm{S}}C_1\cdot g(q_{\mathrm{f}})\right]\geq 1$. As a result, from (40), we need to show that $g'(q_{\mathrm{f}})-g''(q_{\mathrm{f}})>0$. This inequality always holds by deriving and substituting $g''(q_{\mathrm{f}})$ and using the above relationships among parameters.

Since $g(0)=1$ and $g'(0)=1+p_{\mathrm{m}}-\Lambda_{\mathrm{T}}$, according to (39), we need to show that

$$\exp\left(\Lambda_{\mathrm{T}}\lambda_{\mathrm{S}}C_1\right) > \Lambda_{\mathrm{T}}\lambda_{\mathrm{S}}C_1\left(1+p_{\mathrm{m}}-\Lambda_{\mathrm{T}}\right). \tag{42}$$

The Taylor series expansion of $\exp(\Lambda_{\mathrm{T}}\lambda_{\mathrm{S}}C_1)$ can be expressed as

$$\exp\left(\Lambda_{\mathrm{T}}\lambda_{\mathrm{S}}C_1\right) = 1 + \Lambda_{\mathrm{T}}\lambda_{\mathrm{S}}C_1 + \left(\Lambda_{\mathrm{T}}\lambda_{\mathrm{S}}C_1\right)^2\Big/2 + \cdots. \tag{43}$$

Based on (42) and (43), we need to show that

$$\left(\Lambda_{\mathrm{T}}\lambda_{\mathrm{S}}C_1 - p_{\mathrm{m}}\right)^2\Big/2 + \left(1-p_{\mathrm{m}}^2/2\right) + \cdots > -\Lambda_{\mathrm{T}}^2\lambda_{\mathrm{S}}C_1. \tag{44}$$

The above inequality always holds as the left hand side is positive and the right hand side is negative.

In summary, (37) holds and hence retransmission probability q_{f} is a unique solution of the fixed-point equation.

C. Proof of Corollary 1

A queue is said to be stable if its queue length has a limiting distribution as time goes to infinity [40]. The network is stable when the queues of all source nodes are stable. To guarantee the network stability, we consider a dominant network [41], [42], where all source nodes being granted access to the medium and having empty queues make dummy transmissions. The utilization factor of each source node in the dominant network equals to one, i.e., $\rho = 1$, which represents the worst case scenario for interference. As a result, the interferer density is given by

$$\lambda_{\mathrm{I}} = \frac{(1+q_{\mathrm{f}})\,p_{\mathrm{m}}}{1+p_{\mathrm{m}}q_{\mathrm{f}}}\lambda_{\mathrm{S}}. \tag{45}$$

Since the arrival and service processes are ergodic and stationary, by Loynes' theorem [43], the sufficient condition for the network stability is that $\Lambda_{\mathrm{T}} < \mu = p_{\mathrm{m}}/(1+p_{\mathrm{m}}q_{\mathrm{f}})$, where retransmission probability q_{f} is the solution of fixed-point equation (13). Note that (13) is obtained by substituting (45) into $q_{\mathrm{f}} = 1-\exp\left(-\lambda_{\mathrm{I}}\cdot C_1\right)$. Following an argument similar to that in Appendix B, the uniqueness of the solution of (13) can be proved by setting

$$g\left(q_{\mathrm{f}}\right) = \frac{1+q_{\mathrm{f}}}{1+p_{\mathrm{m}}q_{\mathrm{f}}}. \tag{46}$$

D. Proof of Proposition 3

The outage probability of the conventional truncated ARQ scheme can be expressed as

$$\begin{aligned} q_{\text{out}}^{\text{Conv}} &= \mathbb{P}\left(\gamma_{S_0D_0}(t)<\beta, \gamma_{S_0D_0}(t+1)<\beta\right) \\ &\overset{(a)}{=} \mathbb{E}_{\Phi_{\mathrm{I}}(t),\Phi_{\mathrm{I}}(t+1)}\left[\left(1-\prod_{x\in\Phi_{\mathrm{I}}(t)}\eta_{11}\right)\left(1-\prod_{x\in\Phi_{\mathrm{I}}(t+1)}\eta_{11}\right)\right] \end{aligned} \tag{47}$$

where $\Phi_{\mathrm{I}}(t) = \Phi_{\text{em}}(t)\cup\Phi_{\text{reS}}(t)$, $\Phi_{\mathrm{I}}(t+1) = \Phi_{\text{em}}(t+1)\cup\Phi_{\text{reS}}(t+1)$, and (a) follows by taking expectations over the independent fading coefficients between source node S_0 and destination node D_0, and by taking Laplace transforms of the independent fading coefficients between interferers and destination node D_0.

In these two consecutive time-slots, $\Phi_{\text{em}}(t+1)$ is independent of $\Phi_{\mathrm{I}}(t)$ and $\Phi_{\text{reS}}(t+1)$, while $\Phi_{\text{reS}}(t+1)$ is a subset of $\Phi_{\text{em}}(t)$ because of source retransmissions, which leads to the temporal correlation of interference power. As only the source nodes retransmit the packets in the conventional truncated ARQ scheme, λ_{reS} equals to λ_{re}. As a result, we have

$$\begin{aligned} q_{\text{out}}^{\text{Conv}} =& 1-\mathbb{E}\left[\prod_{x\in\Phi_{\mathrm{I}}(t)}\eta_{11}\right]-\mathbb{E}\left[\prod_{x\in\Phi_{\mathrm{I}}(t+1)}\eta_{11}\right] \\ &+\mathbb{E}\left[\prod_{x\in\Phi_{\mathrm{I}}(t)\setminus\Phi_{\text{reS}}(t+1)}\eta_{11}\right]\mathbb{E}\left[\prod_{x\in\Phi_{\text{em}}(t+1)}\eta_{11}\right] \\ &\times\mathbb{E}\left[\prod_{x\in\Phi_{\text{reS}}(t+1)}\eta_{11}^2\right] \\ \overset{(a)}{=}& 1-2\exp\left(-\lambda_{\mathrm{I}}C_1\right)+\left[\exp\left(-\lambda_{\text{em}}C_1\right)\right]^2\cdot\exp\left(-\lambda_{\text{re}}C_2\right) \end{aligned} \tag{48}$$

where (a) follows from the PGFL of the PPP, and C_1, η_{11}, and C_2 are given in (10), (20), and (26), respectively. Note that the temporal correlation of interference power observed by the destination node in two consecutive time-slots is considered by taking a joint expectation over the same set of interferers $\Phi_{\text{reS}}(t+1)$.

E. Proof of Proposition 4

For a typical source-destination pair, Events $\mathcal{E}_{21}$ and $\mathcal{E}_{22}$ can be expressed respectively as

$$\begin{aligned} \mathcal{E}_{21} &= \left\{\gamma_{S_0D_0}(t)<\beta\cap\gamma_{S_0D_0}(t+1)<\beta\right\} \\ \mathcal{E}_{22} &= \left\{\gamma_{S_0R_n}(t)<\beta\cup\gamma_{R_nD_0}(t+1)<\beta, \forall n\in[1,k]\right\}. \end{aligned} \tag{49}$$

Hence, the outage probability of the cooperative truncated ARQ scheme can be expressed as

$$\begin{aligned} q_{\text{out}}^{\text{Coop}} &= \sum_{k=0}^{\infty}\mathbb{P}\left(K_0=k\right)\cdot\mathbb{P}\left[\mathcal{E}_{21}\cap\mathcal{E}_{22}\,|K_0=k\right] \\ &\overset{(a)}{=}\sum_{k=0}^{\infty}\mathbb{P}\left(K_0=k\right)\cdot\mathbb{E}\left[\mathbb{P}\left(\mathcal{E}_{21}\right)\cdot\mathbb{P}\left(\mathcal{E}_{22}\,|K_0=k\right)\right] \end{aligned} \tag{50}$$

where the expectation is taken over the point process of interferers in two consecutive time-slots, and (a) follows from the independence of the fading coefficients for different channels.

Following the similar arguments in (19) and (20), we have

$$\mathbb{P}\left(\mathcal{E}_{21}\right) = \left[1-\prod_{x\in\Phi_{\mathrm{I}}(t)}\eta_{11}\right]\left[1-\prod_{x\in\Phi_{\mathrm{I}}(t+1)}\eta_{11}\right] \tag{51}$$

and

$$\begin{aligned} \mathbb{P}\left(\mathcal{E}_{22}\,|K_0=k\right) &= \left[1-\prod_{x\in\Phi_{\mathrm{I}}(t)}\eta_{22}\cdot\prod_{x\in\Phi_{\mathrm{I}}(t+1)}\eta_{31}\right]^k \\ &= (1-C)^k \end{aligned} \tag{52}$$

where $\Phi_{\mathrm{I}}(t) = \Phi_{\text{em}}(t)\cup\Phi_{\text{reS}}(t)\cup\Phi_{\text{reR}}(t)$ and $\Phi_{\mathrm{I}}(t+1) = \Phi_{\text{em}}(t+1)\cup\Phi_{\text{reS}}(t+1)\cup\Phi_{\text{reR}}(t+1)$ are the sets of interferer locations at time-slots t and $t+1$ respectively, and η_{11}, η_{22}, and η_{31} are given in (20).

By applying the binomial expansion in (52), we have

$$\begin{aligned}&\mathbb{E}\left[\mathbb{P}\left(\mathcal{E}_{21}\right)\cdot\mathbb{P}\left(\mathcal{E}_{22}\left|K_0=k\right.\right)\right]\\&=\sum_{m=0}^{k}\binom{k}{m}(-1)^m\mathbb{E}_{\Phi_{\mathrm{I}}(t),\Phi_{\mathrm{I}}(t+1)}\left[\mathbb{P}\left(\mathcal{E}_{21}\right)\cdot C^m\right]\end{aligned}\tag{53}$$

where the joint expectation over the same set of interferers is taken to incorporate the effect of spatial and temporal interference correlation.

The correlation of node locations, defined in (15) and (16), induces the temporal correlation of interference power in consecutive time-slots t and $t+1$. By transforming the point process of transmitting sources at time-slot t to the point process of retransmitting relays at time-slot $t+1$, and by separating point process $\Phi_{\mathrm{I}}(t)\cup\Phi_{\mathrm{I}}(t+1)$ into independent point processes, we have

$$\begin{aligned}C=&\prod_{x\in\Phi_{\mathrm{I}}(t)\setminus\Phi_{\mathrm{re}}(t+1)}\eta_{22}\cdot\prod_{x\in\Phi_{\mathrm{em}}(t+1)}\eta_{31}\\&\times\prod_{x\in\Phi_{\mathrm{reS}}(t+1)}\eta_{22}\eta_{31}\cdot\prod_{x\in\Phi_{\mathrm{reR}}(t+1)}\eta_{21}\eta_{31}.\end{aligned}\tag{54}$$

Substituting (51) and (54) into (53), we can obtain outage probability $q_{\mathrm{out}}^{\mathrm{Coop}}$ in (27) by applying the PGFL of the PPP.

References

[1] K. S. Gilhousen, I. M. Jacobs, R. Padovani, A. J. Viterbi, J. LA Weaver, and C. E. Wheatley III, “On the capacity of a cellular CDMA system,” *IEEE Trans. Veh. Technol.*, vol. 40, no. 2, pp. 303–312, May 1991.

[2] D. Stoyan, W. Kendall, J. Mecke, and L. Ruschendorf, *Stochastic Geometry and its Applications*. Wiley New York, 1987.

[3] M. Haenggi, *Stochastic Geometry for Wireless Networks*. Cambridge University Press, 2012.

[4] S. Weber, J. G. Andrews, and N. Jindal, “The effect of fading, channel inversion, and threshold scheduling on ad hoc networks,” *IEEE Trans. Inf. Theory*, vol. 53, no. 11, pp. 4127–4149, Nov. 2007.

[5] F. Baccelli, P. Miihlethaler, and B. Blaszczyszyn, “Stochastic analysis of spatial and opportunistic ALOHA,” *IEEE J. Select. Areas Commun.*, vol. 27, no. 7, pp. 1105–1119, Sept. 2009.

[6] C. Zhai, W. Zhang, and G. Mao, “Cooperative spectrum sharing between cellular and ad-hoc networks,” *IEEE Trans. Wireless Commun.*, vol. 13, no. 7, pp. 4025–4037, Jul. 2014.

[7] L. Wang and V. Fodor, “On the gain of primary exclusion region and vertical cooperation in spectrum sharing wireless networks,” *IEEE Trans. Veh. Technol.*, vol. 61, no. 8, pp. 3746–3758, Oct. 2012.

[8] A. Altieri, L. Rey Vega, P. Piantanida, and C. Galarza, “Analysis of a cooperative strategy for a large decentralized wireless network,” *IEEE/ACM Trans. Networking*, vol. 22, no. 4, pp. 1039–1051, Aug. 2014.

[9] S. Cho, W. Choi, and K. Huang, “QoS provisioning relay selection in random relay networks,” *IEEE Trans. Veh. Technol.*, vol. 60, no. 6, pp. 2680–2689, Jul. 2011.

[10] R. K. Ganti and M. Haenggi, “Spatial analysis of opportunistic downlink relaying in a two-hop cellular system,” *IEEE Trans. Commun.*, vol. 60, no. 5, pp. 1443–1450, May 2012.

[11] K. Stamatiou and M. Haenggi, “Random-access Poisson networks: stability and delay,” *IEEE Commun. Lett.*, vol. 14, no. 11, pp. 1035–1037, Nov. 2010.

[12] P. H. Nardelli, M. Kountouris, P. Cardieri, and M. Latva-aho, “Throughput optimization in wireless networks under stability and packet loss constraints,” *IEEE Trans. Mobile Comput.*, vol. 13, no. 8, pp. 1883–1895, Aug. 2014.

[13] P. H. Nardelli, M. Kaynia, P. Cardieri, and M. Latva-aho, “Optimal transmission capacity of ad hoc networks with packet retransmissions,” *IEEE Trans. Wireless Commun.*, vol. 11, no. 8, pp. 2760–2766, Aug. 2012.

[14] O. Simeone, Y. Bar-Ness, and U. Spagnolini, “Stable throughput of cognitive radios with and without relaying capability,” *IEEE Trans. Commun.*, vol. 55, no. 12, pp. 2351–2360, Dec. 2007.

[15] I. Krikidis, B. Rong, and A. Ephremides, “Network-level cooperation for a multiple-access channel via dynamic decode-and-forward,” *IEEE Trans. Inf. Theory*, vol. 57, no. 12, pp. 7759–7770, Dec. 2011.

[16] U. Schilcher, C. Bettstetter, and G. Brandner, “Temporal correlation of interference in wireless networks with Rayleigh block fading,” *IEEE Trans. Mobile Comput.*, vol. 11, no. 12, pp. 2109–2120, Dec. 2012.

[17] R. Ganti and M. Haenggi, “Spatial and temporal correlation of the interference in ALOHA ad hoc networks,” *IEEE Commun. Lett.*, vol. 13, no. 9, pp. 631–633, Sept. 2009.

[18] R. Tanbourgi, H. Dhillon, J. Andrews, and F. Jondral, “Effect of spatial interference correlation on the performance of maximum ratio combining,” *IEEE Trans. Wireless Commun.*, vol. 13, no. 6, pp. 3307–3316, Jun. 2014.

[19] K. Gulati, R. Ganti, J. Andrews, B. Evans, and S. Srikanteswara, “Characterizing decentralized wireless networks with temporal correlation in the low outage regime,” *IEEE Trans. Wireless Commun.*, vol. 11, no. 9, pp. 3112–3125, Sept. 2012.

[20] U. Schilcher, S. Toumpis, A. Crismani, G. Brandner, and C. Bettstetter, “How does interference dynamics influence packet delivery in cooperative relaying?” in *Proc. ACM MSWiM'13*, 2013.

[21] A. Crismani, S. Toumpis, U. Schilcher, G. Brandner, and C. Bettstetter, “Cooperative relaying under spatially and temporally correlated interference,” *IEEE Trans. Veh. Technol.*, vol. 64, no. 10, pp. 4655–4669, Oct. 2015.

[22] R. Tanbourgi, H. Jakel, and F. K. Jondral, “Cooperative relaying in a Poisson field of interferers: a diversity order analysis,” in *Proc. IEEE ISIT'13*, 2013.

[23] Y. Zhou and W. Zhuang, “Opportunistic cooperation in wireless ad hoc networks with interference correlation,” *Peer-to-Peer Netw. Appl.*, 2015, doi:10.1007/s12083-015-0422-3.

[24] S. Weber, J. G. Andrews, and N. Jindal, “An overview of the transmission capacity of wireless networks,” *IEEE Trans. Commun.*, vol. 58, no. 12, pp. 3593–3604, Dec. 2010.

[25] K. Stamatiou and M. Haenggi, “Delay characterization of multihop transmission in a Poisson field of interference,” *IEEE/ACM Trans. Networking*, vol. 22, no. 6, pp. 1794–1807, Dec. 2014.

[26] I. Slivnyak, “Some properties of stationary flows of homogeneous random events,” *Theory of Probability and its Applications*, vol. 7, no. 3, pp. 336–341, 1962.

[27] J. Lee, J. G. Andrews, and D. Hong, “Spectrum-sharing transmission capacity with interference cancellation,” *IEEE Trans. Commun.*, vol. 61, no. 1, pp. 76–86, Feb. 2013.

[28] M. Mohammadi, H. Suraweera, and X. Zhou, “Outage probability of wireless ad hoc networks with cooperative relaying,” in *Proc. IEEE GLOBECOM'12*, 2012.

[29] H. Shan, H. T. Cheng, and W. Zhuang, “Cross-layer cooperative MAC protocol in distributed wireless networks,” *IEEE Trans. Wireless Commun.*, vol. 10, no. 8, pp. 2603–2615, Aug. 2011.

[30] Y. Zhou and W. Zhuang, “Throughput analysis of cooperative communication in wireless ad hoc networks with frequency reuse,” *IEEE Trans. Wireless Commun.*, vol. 14, no. 1, pp. 205–218, Jan. 2015.

[31] G. Mao, B. Fidan, and B. D. Anderson, “Wireless sensor network localization techniques,” *Computer Networks*, vol. 51, no. 10, pp. 2529–2553, Jul. 2007.

[32] Y. Zhou, J. Liu, L. Zheng, C. Zhai, and H. Chen, “Link-utility-based cooperative MAC protocol for wireless multi-hop networks,” *IEEE Trans. Wireless Commun.*, vol. 10, no. 3, pp. 995–1005, Mar. 2011.

[33] P. H. Nardelli, P. Cardieri, and M. Latva-aho, “Efficiency of wireless networks under different hopping strategies,” *IEEE Trans. Wireless Commun.*, vol. 11, no. 1, pp. 15–20, Jan. 2012.

[34] M. Haenggi, “The local delay in Poisson networks,” *IEEE Trans. Inf. Theory*, vol. 59, no. 3, pp. 1788–1802, Mar. 2013.

[35] O. Simeone, U. Spagnolini, Y. Bar-Ness, and S. H. Strogatz, “Distributed synchronization in wireless networks,” *IEEE Signal Process. Mag.*, vol. 25, no. 5, pp. 81–97, Sept. 2008.

[36] F. Baccelli and B. Blaszczyszyn, *Stochastic Geometry and Wireless Networks, Part I Theory*. Now Publishers, vol. 1, 2009.

[37] I. Krikidis, “Simultaneous information and energy transfer in large-scale networks with/without relaying,” *IEEE Trans. Commun.*, vol. 62, no. 3, pp. 900–912, Mar. 2014.

[38] S. K. Bose, *An Introduction to Queueing Systems*. Kluwer Academic/Plenum, 2002.

[39] A. Granas and J. Dugundji, *Fixed Point Theory*. Springer Science & Business Media, 2003.

[40] W. Szpankowski, “Stability conditions for some distributed systems: buffered random access systems,” *Adv. in Appl. Probab.*, vol. 26, pp. 498–515, 1994.

[41] W. Luo and A. Ephremides, “Stability of N interacting queues in random-access systems,” *IEEE Trans. Inf. Theory*, vol. 45, no. 5, pp. 1579–1587, Jul. 1999.

[42] L. Dai, “Stability and delay analysis of buffered ALOHA networks,” *IEEE Trans. Wireless Commun.*, vol. 11, no. 8, pp. 2707–2719, Aug. 2012.

[43] R. Loynes, “The stability of a queue with non-independent inter-arrival and service times,” *Proc. Camb. Phil. Soc.*, vol. 58, no. 3, pp. 497–520, 1962.

Yong Zhou (M’16) received the Ph.D. degree at the Department of Electrical and Computer Engineering, University of Waterloo, Canada in 2015, and the M.Eng. and B.Sc. degrees from Shandong University, China in 2011 and 2008, respectively. Since 2015, he has been a Post-Doctoral Fellow with the Department of Electrical and Computer Engineering, University of British Columbia, Canada. His research interests include cooperative networking, relay selection, and SDN-based resource allocation.

Weihua Zhuang (M’93-SM’01-F’08) has been with the Department of Electrical and Computer Engineering, University of Waterloo, Canada, since 1993, where she is a Professor and a Tier I Canada Research Chair in Wireless Communication Networks. Her current research focuses on resource allocation and QoS provisioning in wireless networks, and on smart grid. She is a co-recipient of several best paper awards from IEEE conferences. Dr. Zhuang was the Editor-in-Chief of IEEE Transactions on Vehicular Technology (2007-2013), and the TPC Co-Chair of IEEE VTC Fall 2016. She is a Fellow of the IEEE, a Fellow of the Canadian Academy of Engineering, a Fellow of the Engineering Institute of Canada, and an elected member in the Board of Governors and VP Publications of the IEEE Vehicular Technology Society.